HHS Public Access

Author manuscript

Radiology. Author manuscript; available in PMC 2020 July 27.

Published in final edited form as:

Radiology. 2019 July ; 292(1): 77–83. doi:10.1148/radiol.2019182599.

Growth Dynamics of Mammographic Calcifications::

Differentiating Ductal Carcinoma in Situ from Benign Breast Disease

Lars J. Grimm, MD,MHS, **Matthew M. Miller, MD,PhD**, **Samantha M. Thomas, PhD**, **Yiling Liu, MS**, **Joseph Y. Lo, PhD**, **E. Shelley Hwang, MD,MPH**, **Terry Hyslop, PhD**, **Marc D. Ryser, PhD**

Departments of Radiology (L.J.G., J.Y.L.), Biostatistics & Bioinformatics (S.M.T., Y.L., T.H.), Surgery (E.S.H.), and Population Health Sciences (M.D.R.), Duke University Medical Center, 40 Duke Medicine Circle, DUMC Box 3808, Durham, NC 27710; and the Department of Radiology (M.M.M.), University of Virginia Health System, 1215 Lee St, Charlottesville, VA 22903.

Abstract

Background: Most ductal carcinoma in situ (DCIS) lesions are first detected on screening mammograms as calcifications. However, false-positive biopsy rates for calcifications range from 30% to 87%. Improved methods to differentiate benign from malignant calcifications are thus needed.

Purpose: To quantify the growth rates of DCIS and benign breast disease that manifest as mammographic calcifications.

Materials and Methods: All calcifications ($n = 2359$) for which a stereotactic biopsy was performed from 2008 through 2015 at Duke University Medical Center were retrospectively identified. Mammograms from all cases of DCIS ($n = 404$) were reviewed for calcifications that were visible on mammograms taken at least 6 months before biopsy. Women with at least one prior mammogram with visible calcifications were age- and race-matched 1:2 to women with a benign breast biopsy and calcifications visible on prior mammograms. The long axis of the calcifications was measured on all mammograms. Multivariable adjusted linear mixed-effects models estimated the association of calcification growth rates with patholo findings. Hierarchical clustering accounted for matching benign and DCIS groups.

Results: A total of 74 DCIS calcifications and 148 benign calcifications were included for final analysis. The median patient age was 62 years (interquartile range, 51–71 years). No significant difference in breast density ($P > .05$) or number of available mammograms ($P > .05$) was detected

Address correspondence to L.J.G. (Lars.grimm@duke.edu).

Author contributions: Guarantors of integrity of entire study, L.J.G., Y.L.; study concepts/study design or data acquisition or data analysis/interpretation, all authors; manuscript drafting or manuscript revision for important intellectual content, all authors; approval of final version of submitted manuscript, all authors; agree to ensure any questions related to the work are appropriately resolved, all authors; literature research, L.J.G., M.M.M., M.D.R.; clinical studies, M.M.M., E.S.H.; experimental studies, L.J.G.; statistical analysis, S.M.T., Y.L., T.H., M.D.R.; and manuscript editing, L.J.G., M.M.M., S.M.T., E.S.H., T.H., M.D.R.

Disclosures of Conflicts of Interest: L.J.G. disclosed no relevant relationships. **M.M.M.** disclosed no relevant relationships. **S.M.T.** Activities related to the present article: disclosed no relevant relationships. Activities not related to the present article: disclosed payment from Abbvie for consultancy. Other relationships: disclosed no relevant relationships. **Y.L.** disclosed no relevant relationships. **J.Y.L.** disclosed no relevant relationships. **E.S.H.** disclosed no relevant relationships. **T.H.** Activities related to the present article: disclosed receipt by institution of NCI Core grant which provided infrastructure support for statistical analysis of cancer projects. Activities not related to the present article: disclosed no relevant relationships. Other relationships: disclosed no relevant relationships. **M.D.R.** disclosed no relevant relationships.

between groups. Calcifications associated with DCIS were larger than those associated with benign breast disease at biopsy (median, 10 mm vs 6 mm, respectively; $P < .001$). After adjustment, the relative annual increase in the long-axis length of DCIS calcifications was greater than that of benign breast calcifications (96% [95% confidence interval: 72%, 224%] vs 68% [95% confidence interval: 56%, 80%] per year, respectively; $P < .001$).

Conclusion: Ductal carcinoma in situ calcifications are more extensive at diagnosis and grow faster in extent than those associated with benign breast disease. The rate of calcification change may help to discriminate benign from malignant calcifications.

Summary

Calcifications associated with ductal carcinoma in situ are more extensive at diagnosis and grow faster than those associated with benign breast disease.

Ductal carcinoma in situ (DCIS) represents approximately 20% of all new breast cancer diagnoses in the United States (1). The majority of DCIS lesions are first detected on screening mammograms where they classically manifest as calcifications. In current practice, biopsy referral of calcifications is based on radiologists' impressions of the morphology and distribution according to the Breast Imaging-Reporting and Data System (BI-RADS) Atlas (2). These features have limited predictive value, with false-positive biopsy rates for calcifications ranging from 30% to 87% (2–6). Furthermore, the interobserver variability for these morphology classifiers is at best moderate (2,7,8). Improved methods to allow differentiation of benign from malignant disease are thus needed.

One unexplored calcification feature is the longitudinal growth rate as evident on serial mammograms. This approach has not been fully investigated because it is standard of care to biopsy all new or growing calcifications that are not definitively benign and to surgically excise those representing atypia or cancer (1). Nevertheless, up to 29% of biopsied cancers can be seen in retrospect on prior mammograms, which provides an opportunity to evaluate the temporal evolution of calcifications (9,10). Filev et al used a data set of retrospectively identified calcifications to develop an automated registration and classification algorithm that differentiates benign from malignant disease based on single-interval changes of calcifications (11). Similarly, Thomson et al used a retrospective data set to demonstrate faster growth rates for high-grade versus low-grade DCIS (12). These prior studies demonstrate the feasibility of identifying retrospective data sets of mammographic calcifications for analysis, as well as the promise of using calcification changes over time for classification purposes.

We hypothesized that DCIS has a faster growth rate than benign breast disease and hence may be a discriminating factor in the evaluation of calcifications. The purpose of this study was to quantify the growth rates of DCIS and benign breast disease that manifest as mammographic calcifications.

Materials and Methods

This retrospective study was approved by the internal review board and is compliant with the Health Insurance Portability and Accountability Act of 1996. Written informed consent was waived.

Study Patients

We retrospectively identified all calcifications (n = 2359) for which a stereotactic biopsy was performed from January 1, 2008, through December 31, 2015, at Duke University Medical Center via a query of our institutional radiology-pathology database. This query consisted of all pure calcifications without associated masses, asymmetries, or architectural distortions and all patients were asymptomatic. The final pathology results from either stereotactic biopsy or subsequent surgical excision (when performed) were as follows: invasive ductal carcinoma (n = 185), invasive lobular carcinoma (n = 9), DCIS (n = 404), lobular neoplasia (n = 48), atypical ductal hyperplasia (n = 168), flat epithelial atypia (n = 39), atypia not otherwise specified (n = 12), and benign breast disease (n = 1484); pathology results were missing for 11 calcifications. The overall malignancy rate was 25%.

Mammograms

The mammograms containing DCIS calcifications were reviewed by either a current breast imaging fellow (M.M.M.) or a fellowship-trained breast radiologist with 3 years of postfellowship experience (L.J.G.). All available digital mammograms preceding the biopsy of DCIS calcifications were reviewed to determine if the biopsied calcifications had already been present. Only DCIS calcifications that were visible on at least one prior mammogram that predated the biopsy by at least 6 months were included. Benign breast calcifications that were also visible on mammograms at least 6 months prior to biopsy were matched 2:1 for race and age with DCIS calcifications. Calcifications initially classified as BI-RADS 3 were included (n = 24). A flowchart of calcifications included for analysis is shown in Figure 1.

Measurements

On each mammogram, the calcifications were measured by one of the radiologists using digital calipers on a clinical work-station (Centricity PACS; GE Healthcare, Chicago, Ill) with high-resolution (5-megapixel) monitors. The longest axis of calcifications, hereafter referred to as size, was measured and used for subsequent analyses. A subset of 50 images was initially measured by both readers and discussed to ensure that the same measurement approach was utilized by both readers, although this is a standardized task used in routine clinical practice. The radiologists measured the calcifications with access to all prior mammograms. The radiologists were blinded to the pathology outcomes. Although the mammogram immediately preceding a biopsy was diagnostic with magnification views, prior mammograms in which the calcifications were already present were often full-field screening views. For consistency, measurements were made on the craniocaudal and/or medio-lateral oblique full-field views on all mammograms. For each case of biopsied calcifications, breast density according to the BI-RADS Atlas was recorded from the mammogram report preceding the breast biopsy.

Statistical Analysis

Characteristics of patients and biopsied calcifications were summarized by using number (percentage), median, and interquartile range (IQR) for categorical and continuous variables, respectively. For the purposes of this study, calcification growth rates refer to the extent of calcifications, rather than the size or number of individual calcifications. Comparisons between the diagnosis groups were made by using the Cochran-Mantel-Haenszel test for matched categorical variables and the stratified Wilcoxon Rank Sum test for matched continuous variables. Multivariable linear mixed-effects models with random intercept and time-to-diagnosis slope were used to estimate the association of final diagnosis with lesion size and growth rate after adjustment for race, age at diagnosis, and breast density. The models included an interaction term between time and diagnosis to determine if the change over time was different for calcifications with final diagnoses of DCIS versus benign breast disease. Hierarchical clustering was used in all models to account for the clustering of calcifications by match number.

Forty-three percent of calcifications included in the study (96 of 222) had a first recorded lesion size of 0 mm because the corresponding mammogram did not show the calcifications. Of note, these 96 calcifications were all still present on at least two subsequent mammograms, as all calcifications were visible for at least two time points. For these calcifications, the start of growth may have occurred at any time between the first (calcification size, 0 mm) and second (positive calcification size) mammogram. To account for this possibility, we used a multiple imputation procedure to predict the time of calcification initiation for these 96 cases (see Appendix E1 [online]). A total of 100 imputed data sets were used in subsequent linear mixed-effects modeling. Due to the skewed nature of lesion sizes, additional models with log- and square-root–transformed response variables were implemented and model selection was performed by using the Akaike Information Criterion. Model fits were evaluated by using a modified R-squared statistic based on the best linear unbiased predictors of the random-effect models. Analyses were stratified by imputation number and estimates were combined by using the PROC MIANALYZE function in SAS (v9.4; SAS Institute, Cary, NC).

To evaluate the dependency of the model conclusions on the above imputation procedure, models that were fit on the original data were compared with those fit on the imputed data. All statistical analyses were conducted by using SAS (S.M.T.). A P value of .05 was considered indicative of statistical significance and no adjustments were made for multiple testing.

Results

The study included 214 women with a total of 222 biopsied calcifications (Table 1); eight women each had two separate biopsies for calcifications that occurred at different time points. The median age at diagnosis was 62 years (IQR, 51–71 years) and 61% (135 of 222) of the women were white. There were 74 DCIS calcifications and 148 benign calcifications included in the final analysis. This corresponds to an 18% (74 of 404) miss rate for DCIS calcifications that were not properly identified as malignant on prior mammograms. Among the 74 DCIS calcifications, the nuclear grade was as follows: six (8%) were low grade, 43

(58%) were intermediate grade, and 25 (34%) were high grade. DCIS was most commonly estrogen-receptor (ER) positive (82%, 61 of 74) and progesterone-receptor positive (80%, 59 of 74). The benign breast calcifications were most commonly reported as fibrocystic changes (55% [82 of 148]) or fibroadenomas (36% [53 of 148]). There were no statistically significant differences in the distributions of breast density ($P = .29$) or number of mammograms ($P = .75$) between the DCIS and benign biopsy cohorts. The median number of mammograms for each case of biopsied calcifications was three in both groups, with a range of two to seven for DCIS and two to six for benign disease. At the time of biopsy, the extent of the DCIS calcifications was larger than that of the benign calcifications (median, 10 mm [IQR, 5–22 mm] vs 6 mm [IQR, 4–10 mm], respectively; $P < .001$).

Growth trajectories were variable in both groups (Fig 2) and exhibited noticeable differences in mean behaviors (Fig 3). Among the three random-effect models used to model the growth trajectories, the log-transformed model yielded the best fit, with a median modified *R*-squared value of 0.78 and a range of 0.76–0.80. Hereafter, we focus on this model (Table 2), with the results of all three models presented in Appendices E2 and E3 (online). Because the effect sizes are not easily interpretable on the logarithmic scale, we instead report the exponentiated model coefficients. The resulting effect sizes in the original scale have the intuitive interpretation of a relative change in long-axis length per unit change of the predictor (13). For instance, the effect size of the time variable is interpreted as a relative growth rate, that is, the percentage change in lesion size per year.

In the multivariable adjusted model, the long-axis extent of DCIS calcifications at the time of biopsy was 69.1% (95% confidence interval [CI]: 29.5%, 120.8%) greater overall than those associated with benign breast disease ($P < .001$). In addition to this main effect, there was a significant interaction effect between disease status (DCIS vs benign) and time ($P = .04$). More precisely, the relative annual increase in the long-axis length of DCIS was 96.2% (95% CI: 71.6%, 224.4%) compared with 67.7% (95% CI: 56.2%, 80.1%) for benign breast disease. Figure 4 shows an example of fibrocystic disease with no appreciable growth in the long-axis extent over 2 years. Figure 5 shows an example of DCIS that increased in extent by 100%, from 3 mm to 6 mm, over 2 years. Age at the time of biopsy affected the long-axis extent of the calcification (1.2% relative increase per year; 95% CI: 0.1%, 2.2%; $P = .03$), but no associations were found with respect to breast density ($P = .29$).

The associations between characteristics of each woman and calcification size in the log-transformed model were corroborated by the natural-scale– and square-root–transformed models (Appendix E2 [online]). Despite their inferior fit, both model alternatives found an interaction effect between disease state and growth rate ($P < .001$ in both). Finally, in a sensitivity analysis, both the natural-scale– and square-root–transformed models were fit to the original, unimputed data set containing 96 first mammograms with a lesion size of 0 mm (Appendix E4 [online]).

Finally, we characterized DCIS growth rates by nuclear grade and ER status (see Appendices E5 and E6 [online]). Dichotomizing nuclear grade into non–high grade (grades I and II) versus high grade (grade III), we estimated annual growth rates of 70.4% (95% CI: 49.3%, 94.5%) for non–high-grade DCIS and 153.1% (95% CI: 90.5%, 236.2%) for high-

grade DCIS. With respect to ER status, we estimated annual growth rates of 84.3% (95% CI: 61.9%, 109.8%) for ER-positive DCIS and 179.9% (95% CI: 80.0%, 335.1%) for ER-negative DCIS. Due to small sizes, the estimates were imprecise and preclude definitive conclusions.

Discussion

The purpose of this study was to quantify the growth rates of ductal carcinoma in situ (DCIS) and benign breast disease that manifest as mammographic calcifications. We hypothesized that DCIS has a faster growth rate than benign breast disease and hence may be a discriminating factor in the evaluation of calcifications. Our results show that DCIS-associated calcifications are overall larger at diagnosis (10 mm vs 6 mm, respectively) and grow faster in extent (96.2% vs 67.7% per year, respectively) than those associated with benign breast disease lesions. In addition, we found that 18% of DCIS calcifications were either missed or not correctly identified as malignant on at least one prior mammogram. To our knowledge, this is the first study that differentiates the longitudinal growth rates of benign and DCIS calcifications. Our findings show that benign breast disease typically grows over time and hence using a threshold of any growth for intervention will necessarily yield benign biopsies. Additionally, the faster yearly growth rates between DCIS and benign disease could be used in a decision model for biopsy referral. The absolute changes in extent are small, but they should be readily apparent to computer vision algorithms, which in combination with other imaging features could provide more refined prediction models.

Our study expands upon the work of two prior studies that have evaluated the use of serial mammograms for calcification analysis (11,12). Filev et al focused on automated regional registration of calcifications from a single prior image without estimating temporal growth rates (11). While the authors did not specify the types of malignancy (DCIS or invasive breast cancer) included for analysis, they demonstrated the ability to differentiate benign from malignant calcifications. Thomson et al used up to three mammograms per patient to model differential growth rates between grades of DCIS (12). Their finding of a faster growth rate for high-grade versus low-grade DCIS, in conjunction with our results, demonstrates the biologic continuum of benign disease through progressively more aggressive DCIS. By using digital mammograms instead of screen-film technology and by including more mammograms per patient (median, three; range, two to seven), our results offer improved temporal resolution with current technology (14). Together, the three studies demonstrate the promise of calcification growth rates as a predictor of biopsy outcomes and future work in this area.

This line of investigation has potential implications for the management of DCIS via active surveillance, which avoids surgical excision for women at low risk of progression to invasive disease. The three current active surveillance trials randomizing low-risk DCIS to surgery or active surveillance recommend mammograms in women every 6–12 months (15–17); however, this imaging interval is not based on detailed DCIS growth models, as such data does not exist. There are some published estimates on doubling times of invasive breast cancers (18,19) but there is very little published information on DCIS growth rates (20). Our results are a first step toward providing these more detailed growth models.

Our study has some limitations. First, by using full-field screening mammograms, the long-axis extent of the calcifications may have been underestimated. Of note, this choice was a trade-off to ensure consistency between mammograms obtained at different points in time (screening vs diagnostic). Second, the size measurements may have been subject to some interobserver variability (2,7,8); however, by blinding the radiologists to the final pathology results during the measurements, we were able to minimize the risk of systematic bias. Additionally, single-reader measurements do not allow for intrareader variability in how the measurements were made. Third, because our study cohorts included only calcifications that were visible in retrospect on prior examinations, calcifications that were larger or with more obvious morphologies at first manifestation were likely filtered out. Fourth, by including only calcifications seen on prior mammograms, there may be a selection bias against women who do not undergo routine screening mammography, such as those with poor-access issues. Additionally, since patients were asymptomatic, women with advanced disease were underrepresented. Finally, we assumed no change in the biologic process producing the calcifications during our study period. The biologic evolution of normal breast tissue to DCIS is poorly understood but it is possible that measurements on mammograms several years prior to biopsy are of DCIS precursor lesions (21,22).

In conclusion, our study demonstrates that microcalcifications associated with biopsy-confirmed ductal carcinoma in situ (DCIS) are overall larger at diagnosis and grow faster than those associated with biopsy-confirmed benign breast disease. Since benign breast disease can also increase in size over time, the “any growth” biopsy threshold used in current practice contributes toward many biopsies yielding benign results. Finally, we estimated that as many as one in five cases of DCIS are missed in retrospect and often missed over several prior examinations. Further work with larger data sets is needed to validate our findings and to define the sensitivity and specificity of various threshold growth rates. However, if a suitable threshold can be identified, slow-growing calcifications could be safely monitored over time, in conjunction with an amended BI-RADS 3, probably benign, designation.

Supplementary Material

Refer to Web version on PubMed Central for supplementary material.

Abbreviations

BI-RADS	Breast Imaging-Reporting and Data System
CI	confidence interval
DCIS	ductal carcinoma in situ
ER	estrogen receptor
IQR	interquartile range

References

1. Virnig BA, Tuttle TM, Shamliyan T, Kane RL. Ductal carcinoma in situ of the breast: a systematic review of incidence, treatment, and outcomes. J Natl Cancer Inst 2010;102(3):170–178. [PubMed: 20071685]
2. Sickles E, D'Orsi C, Bassett LW, et al. BI-RADS: Mammography. Breast Imaging Reporting and Data System: ACR BI-RADS – Breast Imaging Atlas. 5th ed. Reston, Va: American College of Radiology, 2013.
3. Liberman L, Abramson AF, Squires FB, Glassman JR, Morris EA, Dershaw DD. The breast imaging reporting and data system: positive predictive value of mammographic features and final assessment categories. AJR Am J Roentgenol 1998;171(1):35–40. [PubMed: 9648759]
4. Berg WA, Arnoldus CL, Teferra E, Bhargavan M. Biopsy of amorphous breast calcifications: pathologic outcome and yield at stereotactic biopsy. Radiology 2001;221(2):495–503. [PubMed: 11687695]
5. Burnside ES, Ochsner JE, Fowler KJ, et al. Use of microcalcification descriptors in BI-RADS 4th edition to stratify risk of malignancy. Radiology 2007;242(2): 388–395. [PubMed: 17255409]
6. Bent CK, Bassett LW, D'Orsi CJ, Sayre JW. The positive predictive value of BI-RADS microcalcification descriptors and final assessment categories. AJR Am J Roentgenol 2010;194(5):1378–1383. [PubMed: 20410428]
7. Lazarus E, Mainiero MB, Schepps B, Koelliker SL, Livingston LS. BI-RADS lexicon for US and mammography: interobserver variability and positive predictive value. Radiology 2006;239(2):385–391. [PubMed: 16569780]
8. Lee AY, Wisner DJ, Aminololama-Shakeri S, et al. Inter-reader variability in the use of BI-RADS descriptors for suspicious findings on diagnostic mammography: a multi-institution study of 10 academic radiologists. Acad Radiol 2017;24(1):60–66. [PubMed: 27793579]
9. Hoff SR, Samset JH, Abrahamsen AL, Vigeland E, Klepp O, Hofvind S. Missed and true interval and screen-detected breast cancers in a population based screening program. Acad Radiol 2011;18(4):454–460. [PubMed: 21216632]
10. Martin JE, Moskowitz M, Milbrath JR. Breast cancer missed by mammography. AJR Am J Roentgenol 1979;132(5):737–739. [PubMed: 107737]
11. Filev P, Hadjiiski L, Chan HP, et al. Automated regional registration and characterization of corresponding microcalcification clusters on temporal pairs of mammograms for interval change analysis. Med Phys 2008;35(12):5340–5350. [PubMed: 19175093]
12. Thomson JZ, Evans AJ, Pinder SE, Burrell HC, Wilson AR, Ellis IO. Growth pattern of ductal carcinoma in situ (DCIS): a retrospective analysis based on mammographic findings. Br J Cancer 2001;85(2):225–227. [PubMed: 11461081]
13. Vittinghoff E, Glidden DV, Shiboski SC, McCullough CE. Regression Methods in Biostatistics: Linear, Logistic, Survival, and Repeated Measures. 2nd ed New York, NY: Springer, 2005.
14. Pisano ED, Hendrick RE, Yaffe MJ, et al. Diagnostic accuracy of digital versus film mammography: exploratory analysis of selected population subgroups in DMIST. Radiology 2008;246(2):376–383. [PubMed: 18227537]
15. Francis A, Fallowfield L, Rea D. The LORIS trial: addressing overtreatment of ductal carcinoma in situ. Clin Oncol (R Coll Radiol) 2015;27(1):6–8. [PubMed: 25445552]
16. Elshof LE, Tryfonidis K, Slaets L, et al. Feasibility of a prospective, randomised, open-label, international multicentre, phase III, non-inferiority trial to assess the safety of active surveillance for low risk ductal carcinoma in situ - The LORD study. Eur J Cancer 2015;51(12):1497–1510. [PubMed: 26025767]
17. Wong HI, Chen MC, Wu CS, et al. The usefulness of fast-spin-echo T2-weighted MR imaging in nutcracker syndrome: a case report. Korean J Radiol 2010;11(3):373–377. [PubMed: 20461194]
18. Ryu EB, Chang JM, Seo M, Kim SA, Lim JH, Moon WK. Tumour volume doubling time of molecular breast cancer subtypes assessed by serial breast ultrasound. Eur Radiol 2014;24(9):2227–2235. [PubMed: 24895040]

19. Weedon-Fekjaer H, Lindqvist BH, Vatten LJ, Aalen OO, Tretli S. Breast cancer tumor growth estimated through mammography screening data. Breast Cancer Res 2008;10(3):R41. [PubMed: 18466608]

20. Grimm LJ, Ghate SV, Hwang ES, Soo MS. Imaging features of patients undergoing active surveillance for ductal carcinoma in situ. Acad Radiol 2017;24(11):1364–1371. [PubMed: 28705686]

21. Casasent AK, Edgerton M, Navin NE. Genome evolution in ductal carcinoma in situ: invasion of the clones. J Pathol 2017;241(2):208–218. [PubMed: 27861897]

22. Lopez-Garcia MA, Geyer FC, Lacroix-Triki M, Marchió C, Reis-Filho JS. Breast cancer precursors revisited: molecular features and progression pathways. Histopathology 2010;57(2):171–192. [PubMed: 20500230]

Key Points

- Calcifications associated with ductal carcinoma in situ manifest at a larger size and have a higher relative growth rate compared with those associated with benign breast disease (size, 10 mm vs 6 mm, respectively; growth rate, 96% vs. 68% increase per year, respectively [$P < .001$]).
- Since benign breast disease calcifications grow over time, the “any growth” biopsy threshold in current practice results in many biopsies yielding benign results.

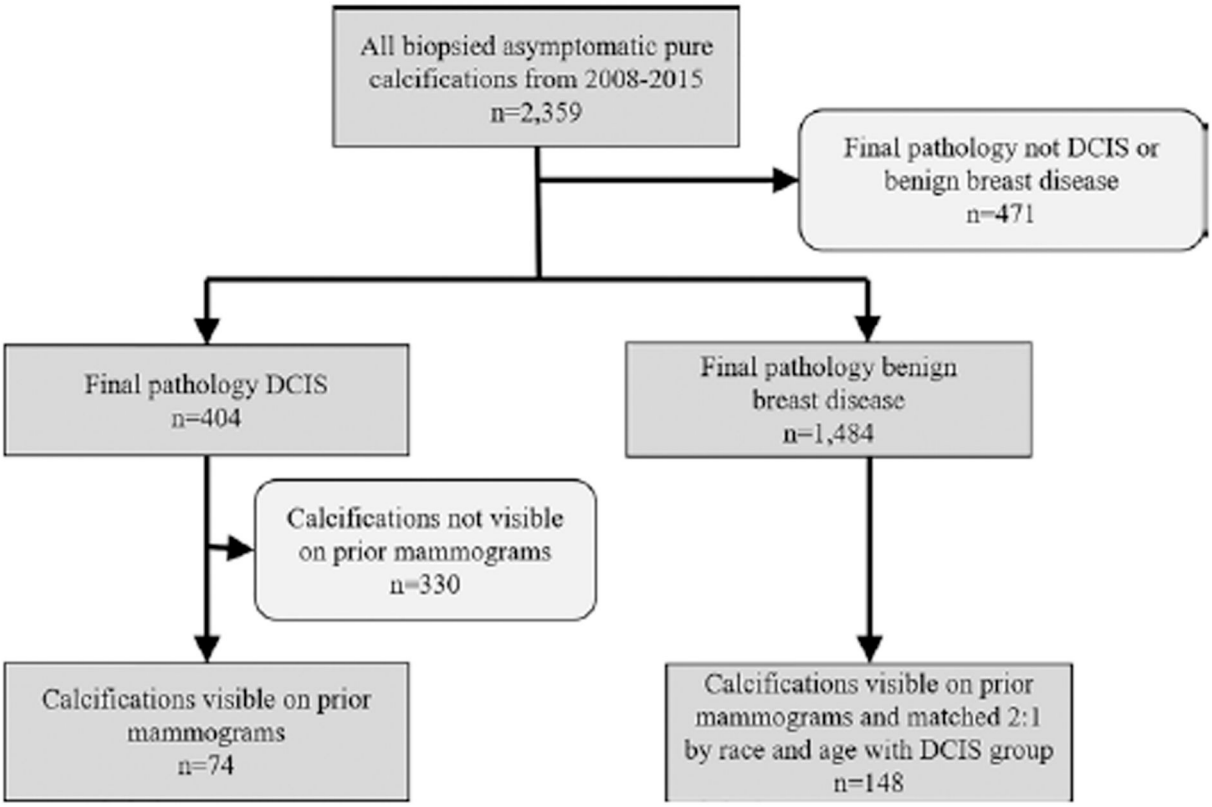

Figure 1:
Flowchart of calcifications representing ductal carcinoma in situ (DCIS) and benign breast disease included in the study.

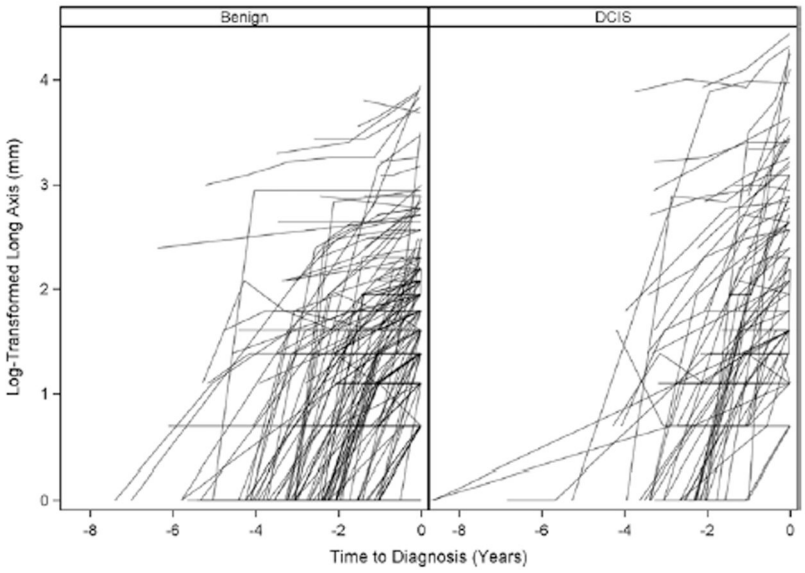

Figure 2:

Log-transformed growth curves for benign breast disease and ductal carcinoma in situ (DCIS). Of note, the 0 values could not be transformed and so were set to zero after the log transformation was applied to the other values.

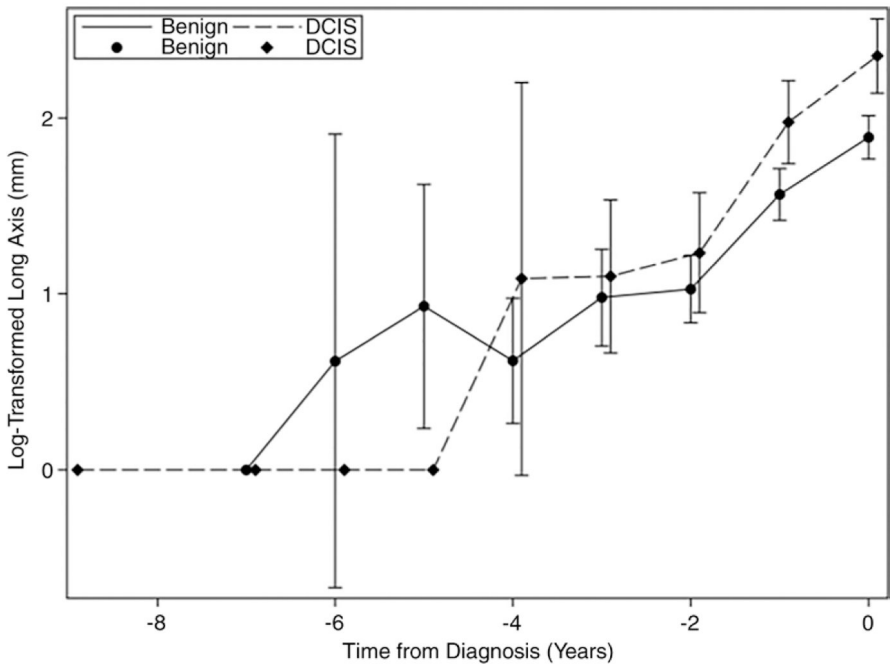

Figure 3:

The mean log-transformed long-axis length over time for ductal carcinoma in situ (DCIS) and benign breast disease, with 95% confidence intervals. The DCIS and benign data points are offset to facilitate visualization. Of note, the 0 values could not be transformed and so were set to zero after the log transformation was applied to the other mean values.

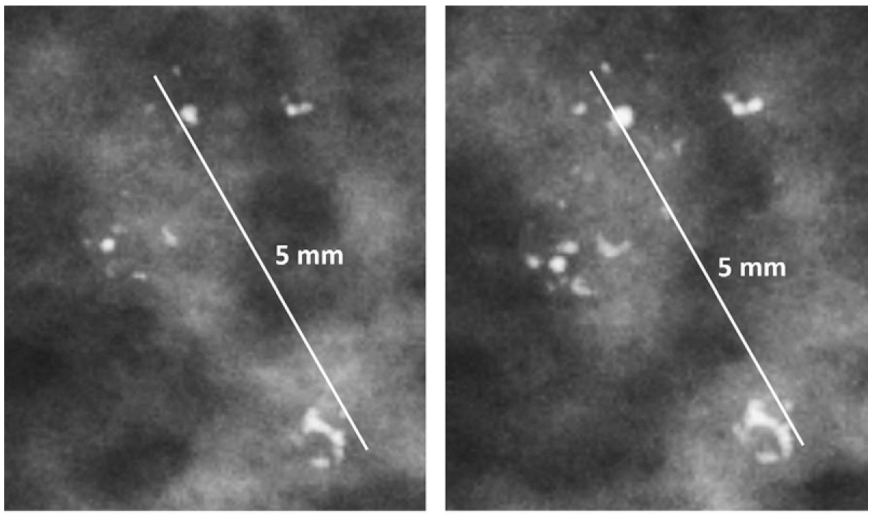

Figure 4:

Mammograms in a 44-year-old woman with calcifications corresponding to fibrocystic disease. **(a)** When first visualized, the calcifications measured 5 mm in long-axis extent; **(b)** 2 years later at the time of biopsy they measured 5 mm.

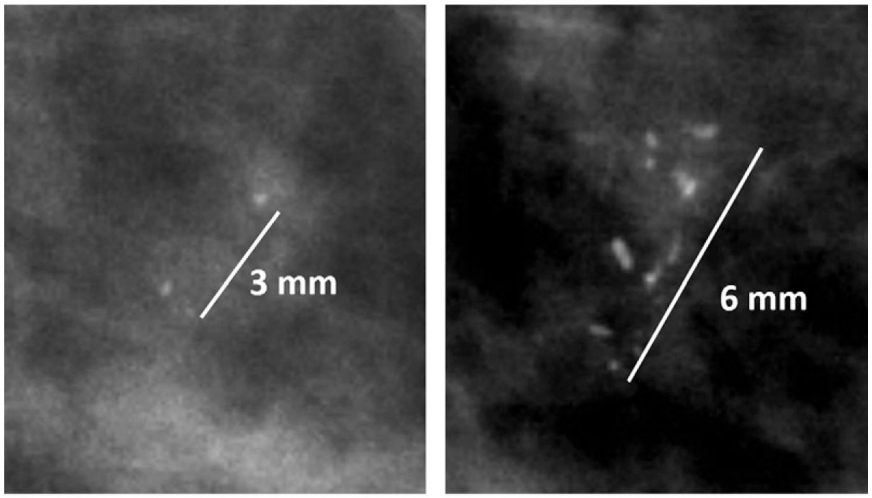

Figure 5:
Mammograms in a 61-year-old woman with calcifications corresponding to intermediate-grade ductal carcinoma in situ. **(a)** When first visualized, the calcifications measured 3 mm; **(b)** 2 years later at the time of biopsy they measured 6 mm.

Table 1:

Characteristics of All Biopsied Calcifications Included in Study

Characteristic	All Calcifications (*n* = 222)	Benign Calcifications (*n* = 148)	DCIS Calcifications (*n* = 74)	*P* Value
Patient age at diagnosis (y) [*,†]	62(32–84) [51–71]	61 (32–84) [51–71]	62 (34–82) [51–71]	…
Long axis at diagnosis (mm) [‡]	7 (4–14)	6 (4–10)	10 (5–22)	<.001
Race [†]				…
White	135 (60.8)	90 (60.8)	45 (60.8)	
Black	87 (39.2)	58 (39.2)	29 (39.2)	
Pathology at diagnosis				…
DCIS	74 (33.3)		74 (100)	
Fat necrosis	2 (0.9)	2 (1.4)	—	
Fibroadenoma	53 (23.9)	53 (35.8)	—	
Fibrocystic changes	82 (36.9)	82 (55.4)	—	
Fibrosis/scar	10 (4.5)	10 (6.8)	—	
Papilloma	1 (0.5)	1 (0.7)	—	
Nuclear grade		…		…
Low	…	…	6(8.1)	
Intermediate	…	…	43 (58.1)	
High	…	…	25 (33.8)	
Estrogen receptor status				…
Negative	…	…	13 (17.6)	
Positive	…	…	61 (82.4)	
Progesterone receptor status				…
Negative	…	…	15 (20.3)	
Positive	…	…	59 (79.7)	
Breast density				.29
Fatty	11(5)	8 (5.4)	3(4.1)	
Scattered fibroglandular	85 (38.3)	61 (41.2)	24 (32.4)	
Heterogeneously dense	110(49.5)	67 (45.3)	43 (58.1)	
Extremely dense	16 (7.2)	12(8.1)	4 (5.4)	

Characteristic	All Calcifications (*n* = 222)	Benign Calcifications (*n* = 148)	DCIS Calcifications (*n* = 74)	*P* Value
No. of mammograms included in analysis[§]				.75
2	49(22.1)	31 (20.9)	18 (24.3)	
3	92 (41.4)	61 (41.2)	31 (41.9)	
4	56 (25.2)	39 (26.4)	17 (23)	
5	17 (7.7)	10 (6.8)	7 (9.5)	
6	7 (3.2)	6(4.1)	1 (1.4)	
7	1 (0.5)	1 (0.7)	0(0)	

Note.—Unless otherwise stated, data are number of calcifications. Data in parentheses are percentages. DCIS = ductal carcinoma in situ.

[*] Data are medians. Data in parentheses are ranges. Data in brackets are interquartile ranges (IQRs).

[†] Variable used in matching.

[‡] Data are medians. Data in parentheses are IQRs.

[§] Includes the mammogram in which the calcifications were first identified prior to a biopsy recommendation.

Table 2:

Mixed-effects Model with Unstructured Covariance and Time-to-Diagnosis Interactions with Imputed Data (100 Imputed Data Sets)

	Linear Mixed-effects Model with Log Transformation of Response	
Effect	**Percent Change***	***P* Value**
Final pathology		
Ductal carcinoma in situ	69 (30, 121)	<.001
Benign	REF	
Time to diagnosis (y)	68 (56, 80)	<.001
Age at diagnosis (y)	1.2(0.1,2.2)	.03
Breast density		
Fatty	−25 (−62, 48)	.40
Scattered fibroglandular	−25 (−54, 21)	.24
Heterogeneously dense	−24 (−52, 21)	.25
Extremely dense	REF	
Race		
Black	9.1 (−14,38)	.47
White	REF	
Time-to-diagnosis interaction		
Ductal carcinoma in situ	17 (0.5, 36)	.04
Benign	REF	

Note.—Unless otherwise stated, data in parentheses are 95% confidence intervals. The response variable (long-axis length) was log transformed prior to model fitting. The variance-covariance estimates of the random effects are shown in Appendix E2 (online). REF = reference standard for calculations.

*For each model coefficient $\hat{\beta}$ estimated on the log-transformed scale, percent change on the natural scale was calculated as $100 \cdot \left(e^{\hat{\beta}} - 1\right)$.